A STUDY OF PROPERTIES OF TYPE IA SUPERNOVA AND THE CALIBRATION OF MULTIBAND PHOTOMETRY

An Undergraduate Research Scholars Thesis

by

DEEPAK BASTOLA

Submitted to Honors and Undergraduate Research
Texas A&M University
in partial fulfillment of the requirements for the designation as

UNDERGRADUATE RESEARCH SCHOLAR

May 2012

Major: Physics
Mathematics

A STUDY OF PROPERTIES OF TYPE IA SUPERNOVA AND THE CALIBRATION OF MULTIBAND PHOTOMETRY

An Undergraduate Research Scholars Thesis

by

DEEPAK BASTOLA

Submitted to Honors and Undergraduate Research
Texas A&M University
in partial fulfillment of the requirements for the designation as

UNDERGRADUATE RESEARCH SCHOLAR

Approved by:

Research Advisor: Kevin Krisciunas
Associate Director, Honors and Undergraduate Research: Duncan MacKenzie

May 2012

Major: Physics
Mathematics

ABSTRACT

A Study of Properties of Type Ia Supernova and the Calibration of Multiband Photometry. (May 2012)

Deepak Bastola
Department of Physics and Astronomy
Department of Mathematics
Texas A&M University

Research Advisor: Dr. Kevin Krisciunas
Department of Physics and Astronomy

The peak luminosity of Type Ia Supernova (SN) can be calibrated using a distance independent luminosity parameter called the decline rate parameter (Δm_{15} (B) to get accurate distances to the galaxies. The photometry gathered from the telescopes should be transformed to a standard scale for uniformity and should be corrected for precision in measurements. The sources of systematic errors are correctly identified and remedied using S-corrections and extinction corrections. The study found a larger scatter in the photometry of Type Ia Supernovae (SNe) in the ultraviolet band (U-band). The importance of Type Ia as a valuable cosmological tool is subsequently shown by deriving the U-band decline rate relation and the magnitude redshift diagram for 36 objects. The photometry of Type Ia SNe puts constraints on the Einstein's equation of state parameters and supports the Dark Energy cosmological parameter causing the accelerated expansion of the Universe.

DEDICATION

This thesis is dedicated to my Dad and Mom, Tika Prasad and Kumari Bastola, whose inspirations have always pushed me towards higher achievements. I would also like to dedicate this achievement to every single circumstance that drove me toward pursuing my studies and research in physics and astronomy.

ACKNOWLEDGMENTS

First and foremost, I would like to thank my research advisor, Dr. Kevin Krisciunas, for providing me a great opportunity to learn about Supernovae and advising me productively in different aspects of the research.

I would also like to thank the Department of Physics and Astronomy, Texas A & M University for providing me a platform to pursue my interest and giving me scholarships to honor my academic achievements. I would also like to use this opportunity to thank the Department of Financial Aid, Texas A & M University for giving me generous financial aids to help ease my financial burdens.

NOMENCLATURE

SN	Supernova
SNe	Supernovae
Ia	Type ‘Ia’
Ib	Type ‘Ib’
Ic	Type ‘Ic’
z	Redshift
nm	Nanometers
Ω_m	Mass density parameter
Ω_Λ	Energy density parameter
γ	Gamma
CCD	Charge coupled device
ADU	Analog-to-digital units
IRAF	Image reduction and analysis facility

TABLE OF CONTENTS

LIST OF FIGURES

FIGURE Page

LIST OF TABLES

TABLE Page

CHAPTER I

INTRODUCTION

A supernova is a star that explodes at the end of its life. Supernovae are classified according to their spectra (Minkowski 1941) as Type I and Type II supernovae. Type II SNe have hydrogen in their spectra. Such an object is believed to be a single, massive star (greater than 8 solar masses) that eventually develops an iron core, and then explodes, leaving behind a neutron star or a black hole. Type I SNe do not have hydrogen in their spectra. They are further subdivided into three subclasses. The prime identifying characteristic of a Type Ia SN is an absorption line of singly ionized silicon, whose rest wavelength is 635.5 nm. These objects are thought to be exploding white dwarf stars - either a single white dwarf with a nearby mass-donating companion, or two white dwarf stars that merge; in both cases the white dwarf accumulates enough material from the companion star to reach the Chandrasekhar Limit of 1.4 solar masses. Type Ib and Ic SNe do not have hydrogen or silicon in their spectra; they are believed to be single massive stars that have been stripped of much of their outer envelopes. Like Type II SNe, Type Ib and Ic objects are core collapse stars that produce neutron stars or black holes. Type Ia SNe occur in all kinds of galaxies, whereas Type Ib and Type Ic have been seen only in spiral galaxies near sites of recent star formation.

This thesis follows the style and format of the Astrophysical Journal.

Type Ia SNe serve as precise cosmological distance indicators because of their high luminosity. The extraordinary finding that the universe is accelerating has invigorated the onset of several new SN search projects aimed at using Type Ia SNe as standardizable candles to improve the determinations of the density parameters (Ω_m, Ω_Λ) and to trace the evolution of the expansion factor through the universe's history (Riello et al. 2005; Leibundgut et al. 2003).The energetic display of supernovae explosions is a result of radioactive decay due to electron capture of ^{56}Ni nucleus with a half-life of 6.1 days (Leibundgut et al. 2003). Energetic γ-photons are emitted in the process and the resulting ^{56}Co isotope, also unstable, decays with a half-life of 77.1 days through electron capture (81%) and β-decay (19%) to ^{56}Fe, again emitting highly energetic γ-photons in the process. The magnitude of a supernova is a logarithmic measure of the brightness which is extensively studied using plots of brightness vs. time.

Light curve

The brightness of the source over time is called a light curve. The light curve of a supernova is derived by plotting its magnitude as a function of time elapsed. The light curve reaches maximum optical brightness 2 to 3 weeks after the supernova explosion. The light curves of all SNe Ia in the blue band basically look the same, and the time corresponding the peak brightness in this band is called the B-band maximum. The mean Type Ia light curve consists of the initial rise and fall of the peak that lasts until 30 days after maximum light, after which they subsequently dim with a fading tail. The SNe Ia light curves, except for a few odd events that can be easily recognized by their spectra,

represent a single parameter family of shapes that can be stretched to a single universal shape, and this universality allows the nature of the individual event to be identified, independent of the distance (Arnett 1999). The brightness information from a supernova explosion is also relatively easy to obtain, and hence, light curves have been one of the mainstays of supernova research (Leibundgut et al. 2001).

Decline rate parameter

SN Ia have a well-established relationship between their optical peak luminosity and the rate of brightness decline, making them excellent standardizable candles (Branch & Tammann 1992; Phillips 1993). The standardizing is done by calibrating the peak luminosity with distance independent observables such as the light-curve shape. The importance of such distance independent luminosity indicators has led to the development of a large number of photometric and spectroscopic methods (Nugent et al. 1995; Wang et al. 2005, 2006; Bailey et al. 2009). One of such measures is the number of magnitudes the B-band declines in the first 15 days after maximum light, Δm_{15} (B), which was first formulated by Phillips (1993); the slower the decline, the greater the peak luminosity (Phillips 1993; Hamuy et al. 1996a; Phillips et al. 1999; Garnavich et al. 2004; Mazzali et al. 2011).

Broadband filters

It is imperative to talk about broadband filter systems and passbands and explain how to obtain correct photometry of a supernova. A passband is a range of frequencies or

wavelengths that can pass through a filter without being cut-off. The ratio of the apparent brightness, or equivalently, the magnitude difference between any two stars depends upon the passband through which they are observed. It is very difficult to compare measurements of stellar objects made by different observers with different equipment and different detectors. So, we define a series of standard passbands, and design equipment to operate in one or more of these passbands. There are five passbands that are commonly used in astronomy- purple, blue, green, orange, and red. The passbands are affected by the earth's atmosphere, telescope optics, filters, and detector types (photographic emulsions, photomultiplier tubes, CCDs, etc.).

A "broadband filter" is an optical passband that covers a sizeable portion of the optical window (UBVRI). The most widely used set is the Johnson- Cousins UBVRI system, which was described in the 1950s by Harold Johnson and modified later by A.W.J, Cousins. In 1990, Michael Bessell introduced a filter transformation system that would correctly reproduce the Johnson-Cousin passbands and SN observers often transform their measurements to Bessell's filter prescriptions. Because broadband filters transmit lots of photons, they are used to detect faint objects even with short exposure times and small telescopes, and this very fact has made them very useful in studying photometric properties of supernovae.

Photometric systems

A photometric standard system is a system of star magnitudes that puts the magnitudes of various objects on a common scale. A standard photometric system involves a standard telescope, standard filter and a standard detector, while a natural photometric system involves the telescope that we use to measure our stars with, the filter system it uses, and the detector it utilizes. For the consistencies in our observations, we need to convert our measurements as observed to a standard system. It is very difficult to (or even impossible) to recreate filter transmission curves that exactly match the standard transmission curves. This constraint has led us to introduce instrumental magnitudes, which can easily be transformed to standard magnitudes.

Instrumental magnitudes

Instrumental and standard star magnitudes in a particular band are related in the following way:

$$M_{standard} = m_{instrumental} + ZP - K * (x) + CT * (color), \quad (1)$$

where ZP, the zero-point, determines the flux level relative to which the magnitudes are defined, the extinction coefficient K describes how the extinction changes with varying airmass, and the color term, CT, describes the color transformation from instrumental system to standard system. Airmass (x) is the ratio of the path length through the atmosphere (y) compared to the path length at the zenith. At a zenith angle z of the position of the star, the value of x is proportional to sec (z).

The star Vega is defined to have a magnitude of zero and is thus a reference point in calculating apparent magnitudes of stars, commonly called zeropoint. Equation 1 assumes a linear correlation exists between instrumental colors and standard colors, but this is only true when the instrumental filter transmission curves are close to the standard ones. To transform instrumental magnitudes to standard magnitudes, we need to observe our objects in at least two filters.

Color

The term "color" is defined as the difference of two magnitudes of a luminous object through two filters in the standard system or a natural system. The relation between instrumental color and the magnitudes of a star is also similar to the above relation (1) and is given in the V-band (say) by:

$$V = v + CT_v\,(b - v) - K_v*(\sec(z)) + ZP_v, \qquad (2)$$

where the terms V, v and b-v are the standard magnitude, instrumental magnitude, and instrumental color of V-band respectively. If we use a blue filter in our camera, we would measure only the blue light emitted by the stars; hence, hot stars would appear brighter than the cool ones. On the other hand, if we use a red filter in our camera, the cool star would appear brighter than the hot one.

Photo detectors

The advent of CCD technology has made supernova searches more systematic and automatic. A CCD camera contains millions of individual picture elements (pixels), each

of which has its own sensitivity to light. A CCD chip is cooled either thermoelectrically or with liquid nitrogen to cut down on noise. Photons are converted into electrons in the chip and are read out as analog-to-digital units (ADU's, or counts). A typical camera and its readout electronics have a limit of 32,767 or 65,535 counts. The zero level of the chip is usually offset by a few hundred counts to make sure that the signal measured is always a positive number. This is known as the "bias level" of the chip and is typically determined by taking a set of 10 frames with zero exposure time. They are combined for a given night into a median bias frame which would later be subtracted from our field images.

Because every pixel has its own sensitivity, we must make "flat frames" to divide the images by, which accounts for the different sensitivities of the pixels. A set of images in each filter is taken. These can be images of an artificially illuminated white spot in the dome during the day (domeflats), or images of the twilight sky obtained right after sunset or right before sunrise. If twilight images are taken, the telescope must be offset by, say, 30 arc seconds between images so that any stars in the frames are located at different locations in the various images.

CHAPTER II

METHODOLOGY

I have completed a set of data on the photometry of the supernova 2003hv and four other field stars from 1 day to 63 days after B- band maximum from the CTIO 0.9m, the CTIO 1.3m, and the Las Campanas 1.0m telescopes in Chile. I performed the initial and intermediate steps of data reduction within the IRAF data reduction environment. IRAF is distributed by the National Optical Astronomy Observatory, which is operated by the Association of Universities for Research in Astronomy, Inc., under cooperative agreement with the National Science Foundation (NSF). Within the ccdred package I used the program *zerocombine* for combining bias frames, *flatcombine* for combining domeflats or twilight sky flats, and *ccdproc* for trimming, bias subtraction and division by flats. Within the digiphot package I used the program *apphot* for obtaining instrumental aperture magnitudes of stars, *photcal* for determining atmospheric extinction, photometric color terms, and photometric zeropoints using standards from Landolt (1992, 2007). The *evalfit* program was used to apply the transformation equations given in (1) to instrumental magnitudes of the program objects (such as supernovae) and the magnitudes of such objects are obtained on the Landolt photometry system.

There is also a complicating factor that we need to be wary of. If the supernova is buried in the light of its host galaxy, the image subtraction templates obtained before the SN blew up in its host should be used, or these image subtracting templates must be

obtained a year or more after the SN is at maximum light. For many objects, this extra step is crucial for obtaining accurate light curves. Once a master bias frame and N flats are made for the N filters used for observing, then the IRAF program *ccdproc* is invoked to trim the data images (the outer couple columns or rows often have strange signal levels), and the images are bias subtracted and flattened. Then the aperture photometry of standard stars of known brightness and color is done using the package *apphot*. The package *photcal* is used to obtain transformation equations from standard stars. Finally, science with the light curves of the supernovae is done from observations made over weeks or months.

The broad band UBVRI photometric observations of SN 2003hv presented here were carried out on 15 dates during 10 September 2003 to 17 October 2003 by my thesis advisor. The observations were made from the Cerro Tololo Inter-American Observatory using ANDICAM (an instrument containing optical and near-IR filters). Leloudas et al. (2009) have already published data from the CTIO 0.9m and Las Campanas 1.0 m telescopes (Leloudas et al. 2009). The supernova was discovered a day before maximum i.e., 2452891.7 JD. Our observed set of data ranged from 2452892.88 JD to 2452953.72 JD and is given in Table 1. Throughout this paper, the phase of the SNe is defined as the time in days from the B-band maximum.

The brightness range of SNe 2003hv was wide, which necessitated the calibration of both relatively bright and faint local sequence stars (Leloudas et al. 2009). In the finder

image the field stars are labeled as star 3, 4, 5, and 15 in Figure 1. The local faint stars were calibrated using the standard star field TPhe observed on photometric conditions on 4 nights in 2003. Flux calibration of the spectra was performed by means of spectrophotometric standard stars observed at similar air mass on the same night as the SN. The SNe was positioned on the outskirts of the galaxy, with no considerable host galaxy extinction. The uncertainties were calculated by combining in quadrature the Poisson photon errors, the read-out noise errors from the pixel within the aperture and the errors in the aperture corrections (Leloudas et al. 2009). We used mean color terms determined on 5 photometric nights in August to October 2003. The transformation from the instrumental magnitudes to the standard Johnson UBV (Johnson et al. 1966) and Kron-Cousins RI (Cousins 1981) systems was established using equation (1).

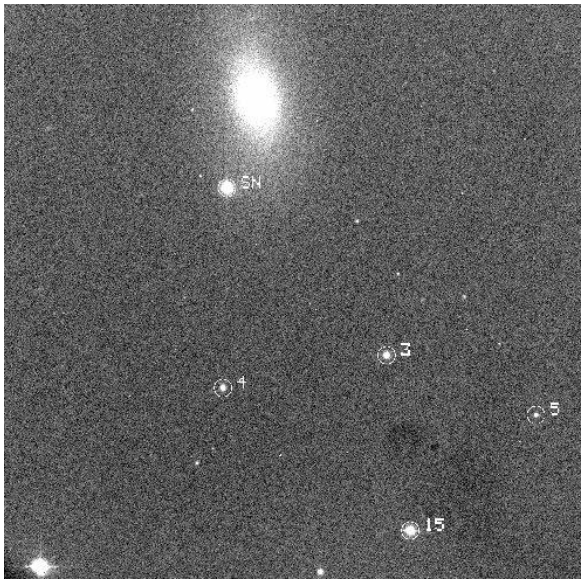

Figure 1. A V-Band finding chart of SN 2003hv with the field stars labeled by numbers.

The significant source of observational bias occurs due to the dust extinction in SN host galaxies. Though SN 2003hv has no considerable host-galaxy extinction, I include the discussion of galaxy extinction to a greater detail for 35 other SNe that we consider here. I used the B-band decline rates of 31 different objects all out to a redshift greater than 0.01 observed by Harvard-Smithsonian Center for Astrophysics (CfA) as presented on Hicken et al. (2009) and plotted them against their extinction corrected U-band peak magnitude to derive a complete U-band decline rate relation. I also added SNe 2003hv, SNe 1999ee, 2000ca, 2001el, and 2004S, observed with the CTIO 0.9-m and ANDICAM to the decline rate curve. The Hubble diagram, also called magnitude-redshift relation, of these SNe is subsequently derived and then a brief cosmological and mathematical implication of my finding about Type Ia SN is discussed near the end of this paper.

CHAPTER III

RESULTS AND DISCUSSIONS

I primarily focus on the U-band photometry of SN 2003hv and enumerate various ways of doing science with the photometry that I derive. SN 2003hv is a fast declining supernova that reached an apparent B-band magnitude of 12.45 mag. It was the brightest supernova discovered in 2003, and one of the brightest supernovae discovered over the past decade (Leloudas et al. 2009). The SNe2003hv was unreddened in its host (Krisciunas 2003). It had a decline rate of Δm_{15} (B) = 1.61 ± 0.02. The distance modulus of SN 2003hv is estimated to be μ_{SN}=31.37±0.05 mag from the method of surface brightness fluctuations (Tonry et al. 2003, Jensen et al. 2003).

The fast decliners SNe are less luminous than slow decliners in the optical band. The observable trend that more luminous SNe have wider light curve that has scatter is mainly due to the differences in the progenitor mass or metallicity (Timmes et al. 2000) or asymmetries (Kasen et al. 2009). Meikle (2000) and Krisciunas et al. (2004) found that SN Ia might serve as a standard candle in the near infrared (IR: JHK bands). Jha et al. (2007) have shown that U-band light curves of SN Ia are standardizable, similar to the optical, and can be used to determine the extinction and distances to their host galaxies. Kessler et al. (2009) have found discrepancies in the determination of cosmological parameters when including the nearby SNe measured in the U-band, the source of which is not clearly known, underlying the importance of understanding SN Ia behavior in this regime.

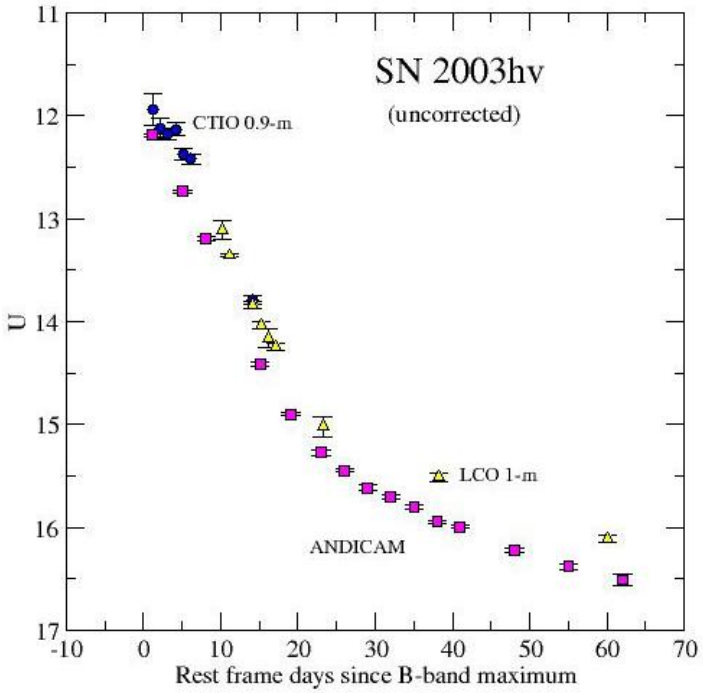

Figure 2. The uncorrected U-band light curve of SN 2003hv.

Discrepancies of up to 0.4 mag in the U-band absolute magnitude are found in the photometry of SNe 2003hv with different telescopes, which is shown in Figure 2. The method of S-correction is one of the prime remedial methods for the discrepancies seen. S-correction stands for spectroscopic correction and is brought upon by combining data obtained with different telescopes and also accounts for the differences in filter shapes (Stritzinger et al. 2002). The S-correction method assumes that the Spectral Energy Distribution of SNe is sufficiently similar and the response of the instruments used for the observation is known.

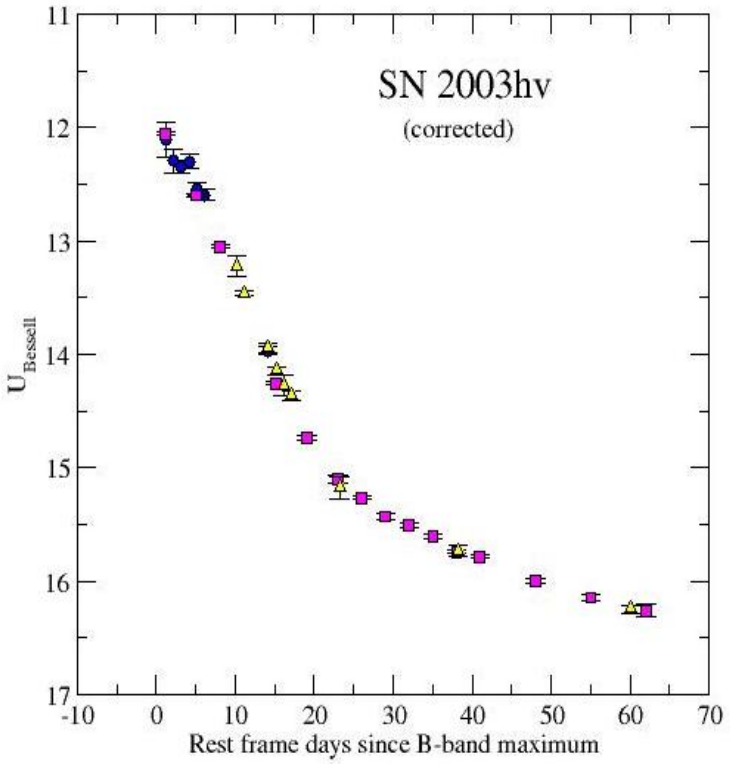

Figure 3. The S-corrected U-band light curve of SN 2003hv.

The K-correction is the difference between the observed magnitude of the redshifted spectrum and the observed magnitude of the rest frame spectrum plus the flux-dilution factor 2.5log (1+z) (Oke & Sandage 1968). However, we did not calculate K-corrections for the U-band because these are negligible compared to the S-corrections. We used the spectra data of SNe 2002bo at four different epochs, including a pre-maximum spectrum to compute the S-correction and to transform the U-band photometry of SN2003hv into Bessell (1990) system. The S-corrected U-band light curve of SN 2003hv is shown in Figure 3, where the brightness of the supernova in the U-band is plotted against the rest-

frame time elapsed since the supernova explosion in days. The final calibrated UBVRI magnitudes, after performing S-corrections, are presented in Table 1.

SN Ia shows a color evolution through the maximum phase. This intrinsic color of a SNe is reddened and theoretically, this is understood as increased line blanketing in the higher-velocity SNe, depressing the B-band flux relative to the V -band flux and causing a redder B − V color (Foley et al. 2009). B − V curve is simply the difference between the B and V light curve. Near maximum SNe Ia redden rapidly, which causes them to reach U maximum about 2.8 days before and V maximum about 2.5 days after B maximum (Branch & Tammann 1992). The intrinsic color is often used to determine the amount of reddening towards the SNe because it appears to be very uniform (Phillips et al. 1999).

The morphology of the U-band light curve resembled that of a normal Type Ia SN, although we lack enough data points to tell exactly the shape before the maximum light. Using the fitting method described in Burns et al. (2009), the host galaxy reddening was found to be E_{B-V} host=-0.04±0.01 mag, with an additional systematic uncertainty of ±0.06 mag due to the observed color spread (Leloudas et al. 2009).

The light curve fit of SN 2003hv shows a B-band decline rate $\Delta m_{15}(B)$ of 1.61±0.02 mag, therefore placing the SN at the faint end of the normal luminosity vs. decline rate distribution, close to the subluminous SN 1991bg-like SN Ia (Fillipenko et al. 1992,

Leloudas et al. 2009). SN 2003hv falls between the decline rate range Δm_{15} (B) of 1.5 to 1.7, making it one of the few to fall in that range.

The use of extinction corrections to our decline rate relation is crucial to the cosmological implication of our findings, and we hence discuss it to show that U-band photometry can lead us to conclusions with significant cosmological importance. The measurement of extinction suffered by a SN can be estimated either by the availability of the SN light curve in at least two pass-bands (around maximum light or between 30 and 90 days past B-band maximum) or at least one spectrum with good signal to noise ratio (Riello et al. 2005). It has been widely known that different line of sight in the galaxy gives different values of extinction coefficients. To correct our data for host galaxy extinction, the intrinsic color (B-V) at maximum and the value of R is needed and is given by $R_V = A_V / E_{B-V}$, where $A_\lambda / A_V = (a*\lambda + b*\lambda) / R_V$ (Cardelli et al. 1989). Normal galactic dust has R_V of 3.1. Observing Type Ia SNe in rest frame optical bands plus one or more near- IR bands allows one to determine R_V and A_V with considerable accuracy (Krisciunas et al. 2007).

Interstellar extinction shows a large range of variability from one line of sight to another, the wavelength dependence of which is well documented in the UV ($0.09\ \mu m < \lambda < 0.32\ \mu m$). According to the Cardelli et al. (1989) , for a unit extinction in V, there is a factor of 1.569 extinction in U and the extinctions in U and B can be formulated in similar form using the relations $R_B = A_B / E_{B-V}$ and $R_U = A_U / E_{U-B}$. Equivalently, the extinctions

in U can be expressed as $E_{U-B} = A_U - A_B$. A powerful test for R is in principle provided by a plot of (B − V) measuring the color excess versus (B − H) measuring the extinction A_B, because A_H is small ($A_H = 0.11A_B$) (Elias et al. 1985). We used the scaling factor derived from the above relations to correct our U-band absolute magnitudes in our U-band decline rate relation.

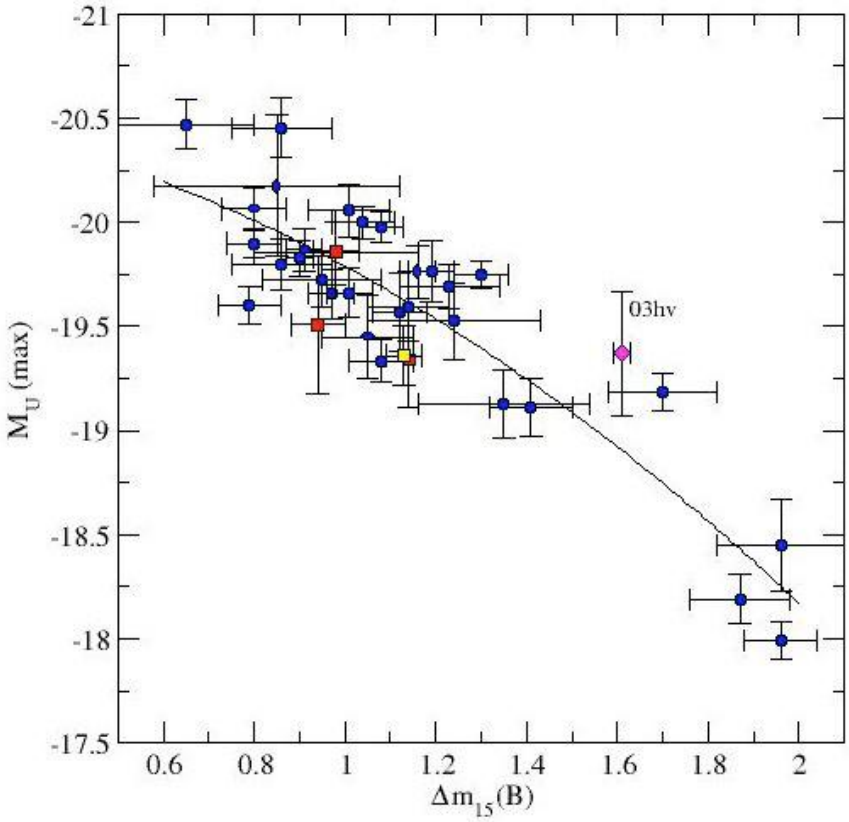

Figure 4. The U-band decline rate relationship of 36 objects including 31 objects from Hicken et al. (2009). SN 2003hv is labeled in the figure, with Δm_{15} (B) = 1.61 ± 0.02 mag

For our purpose of correcting the extinction of the supernovae in our U-band decline relation, we have used R_V=1.7 to reproduce the graph of Hicken et al. (2009, Fig 27). The resulting diagram of the U-band decline rate relation plotted with extinction corrected U-band absolute magnitudes vs. the B-band decline rate parameters is represented in Figure 4. The RMS scatter is ±0.25 mag which compares to ±0.15 mag for BVRI-JHK decline rate relations.

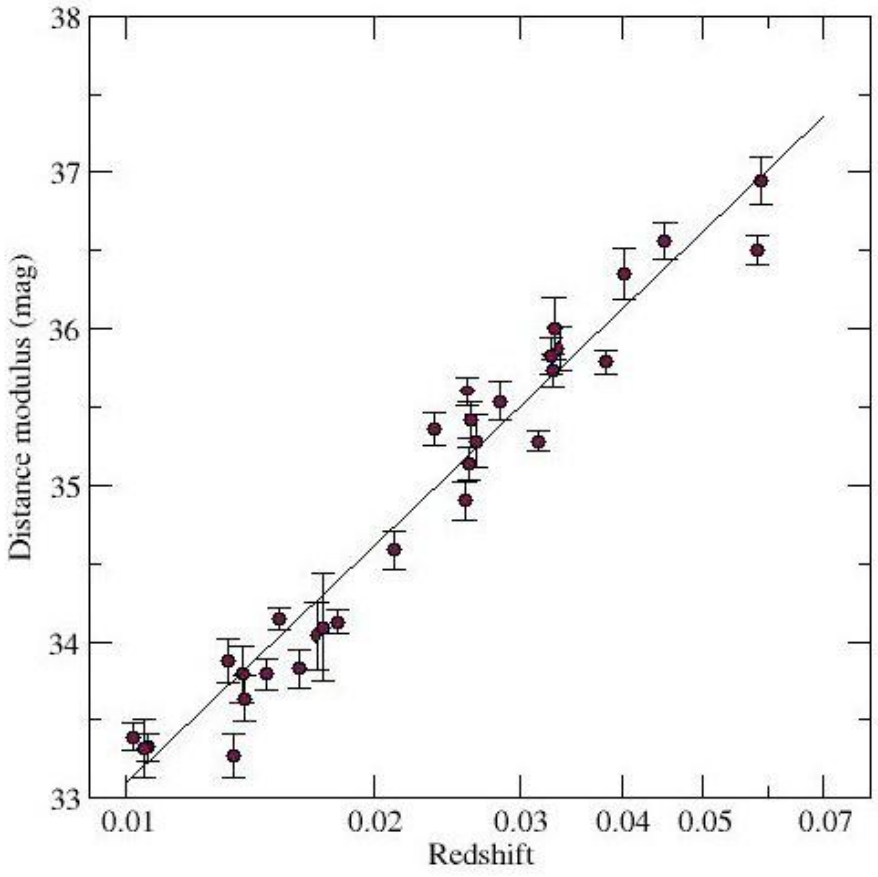

Figure 5. Hubble diagram of 31 Type Ia SNe from Hicken et al. (2009). The RMS scatter is ± 0.24 mag.

In a Hubble diagram for Type Ia SNe, i.e. in a plot of log v_o versus the apparent magnitude, the scatter is not only due to the intrinsic scatter in absolute magnitude but also due to peculiar motions, to extinctions in the parent galaxy, and to observational magnitude errors. I used the distance modulus of the 31 SNe as a function of apparent magnitude vs. the redshift as a function of the velocity and derived a Hubble diagram that is shown in Figure 5. The absolute magnitudes (mU), decline rate parameter $\Delta M_{15}(B)$, the extinction correction factor (E_{U-B}), and the errors in them are enumerated in Table 2. The RMS scatter on our Hubble diagram is +/- 0.24 mag. If we add more distant objects (to redshift ~0.4) we can begin to measure of the effect of Dark Energy on the expansion of the universe, the extent of which is depicted in Figure 6. Relatively nearby SNe Ia ($z \leq 0.1$) will be used to probe departures from pure Hubble flow and to measure the value of the Hubble constant. More remote SNe Ia ($z \leq 1.0$) will be used to test the reality of the universal expansion and measure the acceleration parameter of the universe. The study of SNe at $z \sim 0.1$ is more important for cosmology since the redshift is large enough that the peculiar motions do not introduce dispersion in the Hubble diagram (Ruiz–Lapuente 2003).

The intrinsic variation of SNe Ia is written as a linear relationship given in the B-band (say) as,

$$M_B = - M_{Bt} + \alpha [\Delta m_{15} (B) - \beta] + 5 \log (H_o / 65) \quad (3)$$

where, Δm_{15} (B) is the decline rate parameter, the value of α as well as the dispersion of that relation have been evaluated in samples presented in Phillips et al. (1999) that are

evaluated since 1993, M_{Bt} is the absolute magnitude in B for a template SN Ia of β rate of decline.

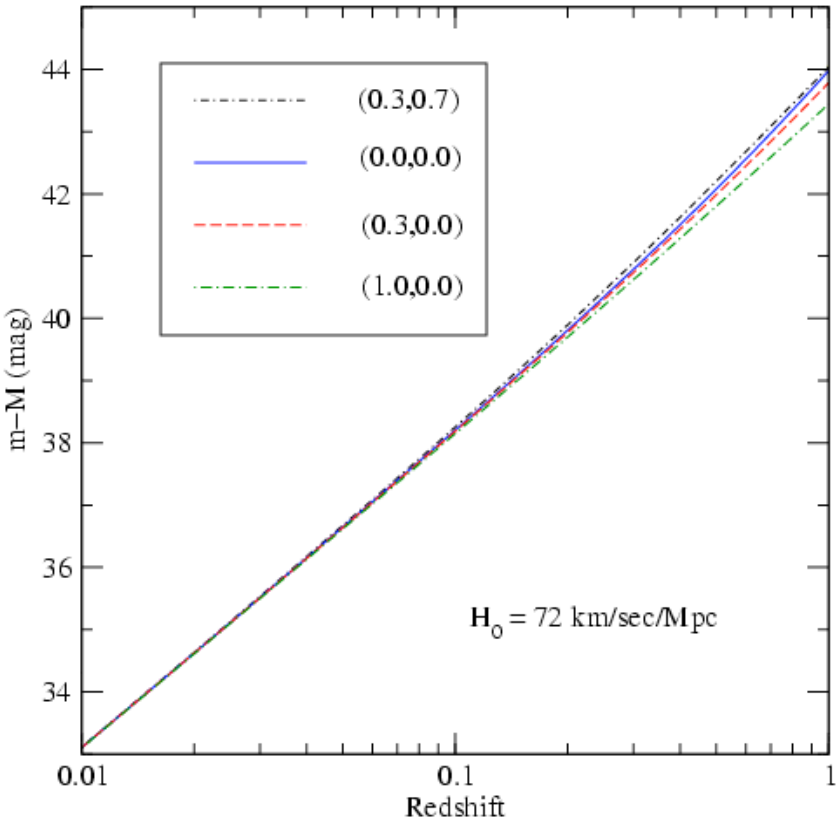

Figure 6. Hubble diagram out to a redshift of 1.0. The line (0.3, 0.7) depicts a model with $\Omega_M = 0.3$ and $\Omega_\Lambda = 0.7$, (0, 0) depicts an empty universe model, (0.3, 0) depicts an open model, and (1.0, 0) depicts a critical density model without any Dark Energy.

I would further like to develop some theoretical insight into the cosmological model of the universe we currently live in. The cosmological principle that makes definite predictions about all unobservable regions beyond the observable universe is given by Robertson-Walker (RW) geometry with metric,

$$ds^2 = -dt^2 + a^2(t) * g_{ij} * dx^i * dx^j, \quad (4)$$

where t is the cosmic time and g_{ij} is the spatial metric on the constant time hypersurfaces, which are homogeneous, isotropic, and thus of constant curvature. This metric is reduced to a single function of time, the scale factor, a, which implies that there is a one to one mapping between the cosmic time and the redshift z,

$$1 + z = a_o / a\,(t), \tag{5}$$

if the expansion is monotonic.

We can study the properties of the scale factor, a, from the Einstein equations which reduces for the RW metric to the Friedmann equations,

$$H^2 = \frac{8\pi G}{3}\rho - \frac{K}{a^2} + \frac{\Lambda}{3}, \tag{6}$$

$$\frac{\ddot{a}}{a} = -\frac{4\pi G}{3}(\rho + 3P) + \frac{\Lambda}{3}, \tag{7}$$

where $H = \dot{a}/a$ is the Hubble function and $K = 0, \pm 1$ is the curvature of the spatial sections. G and Λ are the Newton and cosmological constraints, ρ and P are respectively the energy density and pressure of the cosmic fluids and are related by,

$$\dot{\rho} + 3H(\rho + P) = 0. \tag{8}$$

We can define dimensionless density parameters as,

$$\Omega = \frac{8\pi G\rho}{3H^2}, \qquad \Omega_\Lambda = \frac{\Lambda}{3H^2}, \qquad \Omega_K = -\frac{K}{(Ha)^2}, \tag{9}$$

respectively, for the matter, the cosmological constant, and the curvature. Then, the first Friedmann equation (6) can be written as,

$$E^2(z) = \left(\frac{H}{Ho}\right)^2 = \Omega_{rad}(1+z)^4 + \Omega_M(1+z)^3 + \Omega_K(1+z)^2 + \Omega_{\Lambda,} \quad (10)$$

with $\Omega_K = 1 - \Omega_{rad} - \Omega_M - \Omega_\Lambda$, and E(z) is a function of all the background observables like luminosity distance, angular distance etc. In this scenario, the Dark Energy is well defined and reduces to a single number equivalent to a fluid with equation of state,

$w = P/\rho = -1.$ (11)

There is insurmountable evidence that our astronomical data agrees with the theoretical model just stated. The small dispersion of Type Ia SNe at maximum light (≤ 0.3 mag) and their high absolute luminosity ($M_B \sim -19.3$ mag) makes these objects ideal standard candles with which we try to determine cosmological parameters like $H_{o,}$ Ω_M, Ω_Λ etc. The flux reaching us observers at a redshift z=0 from an object of absolute luminosity, L located at a redshift z is given by the relation,

$$F = \frac{L}{4\pi d_L^2} \ . \quad (12)$$

Goobar and Perlmutter (1995) showed that it is possible to constrain the regions of allowed values in the Ω_M - Ω_Λ plane observationally. It is done by using the magnitude-redshift relation m (z) of a sample of high-z SNe Ia at different z as a function of Ω_M and $\Omega_{\Lambda.}$ The relation is given as,

$m(z) = M + 5\log[d_L(z, \Omega_M, \Omega_\Lambda)] - 5\log(Ho) + K_C + 25,$ (13)

where M is the absolute magnitude of the Supernova, d_L is the luminosity distance, and K_C is the K-correction. In real sense, eq. (12) translates as the magnitude-redshift relation between the apparent magnitude m of an object and its absolute magnitude M in

eq. (13). The luminosity distance, $d_{L,}$ to a source at a redshift z depends crucially upon both the curvature of space and the matter content of the universe,

$$d_L(z) = \frac{(1+z)c\,H_o^{-1}}{|\Omega_{Tot}-1|^{1/2}}\,S(\eta_o - \eta), \tag{14}$$

$$\text{where } \eta_o - \eta = |\Omega_{\text{Tot}} - 1|^{1/2} \int_0^z \frac{dz'}{h(z')}, \tag{15}$$

$$S(x) \text{ is defined as, } \begin{cases} S(x) = \sin(x) \text{ if } K = 1 & (\Omega_{\text{Tot}} > 1) \\ S(x) = \sinh(x) \text{ if } K = -1 & (\Omega_{\text{Tot}} < 1) \\ S(x) = x \text{ if } K = 0 & (\Omega_{\text{Tot}} = 1) \end{cases}, \tag{16}$$

$$\text{and } h(z) = \frac{H(z)}{H_o} = (1+z)\left[1 - \Omega_{Tot} + \sum_\alpha \Omega_\alpha (1+z)^{\gamma_\alpha 1/2}\right] \tag{17}$$

is the dimensionless Hubble parameter, where $\Omega_{Tot} = \sum_\alpha \Omega_\alpha$, $\gamma_\alpha = 1+3w_{\alpha.}(1+z)$ is the cosmological redshift parameter as given by equation (5) and $w_\alpha = \frac{P_\alpha}{\rho_\alpha}$ is the equation of state ($P = -\rho$ by equation (11)) for a Dark Energy cosmological constant.

Two important collaborations in 1998/1999 independently presented the results on the Ω_M - Ω_Λ plane that implied $\Omega_\Lambda > 0$ at a 3σ confidence level as shown in Figure 7. The result from the Supernova Cosmology project gave $\Omega_M = 0.28^{+0.09}_{-0.08}\,(\text{Stat})^{+0.05}_{-0.04}(\text{Syst})$, and that from the High-Z Supernova team gave $\Omega_M = 0.24 \pm 0.1$, for a flat universe model ($\Omega_{Tot} = 1$) (Riess et al. 1998, Perlmutter et al. 1999). So, based on the observations from Type Ia SNe, we can say that the universe contains about 20-30% of its density content as matter and the 70-80% as cosmological constant.

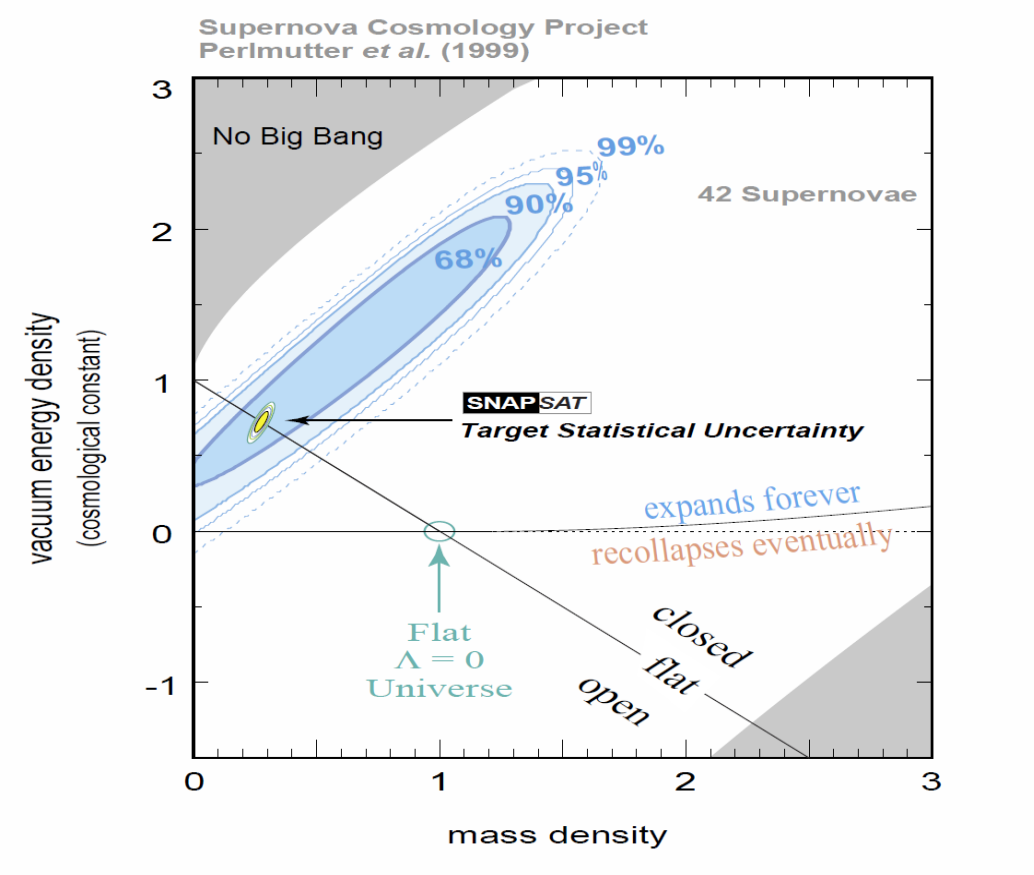

Figure 7. Confidence regions in the Ω_{M}. Ω_{Λ} from 42 high redshift SNe Ia taken from Perlmutter et al. (1999).

CHAPTER IV

CONCLUSION

We can derive various useful relations from the photometry of Type Ia SNe that are of considerable importance both in astrophysics and cosmology. Type Ia SNe are the best known and extensively studied cosmological distance indicators. The U-band photometry of Type Ia SNe shows more scatter in their decline rate relations, but using corrections to our photometry such as S-corrections and extinction corrections one can significantly reduce the systematic errors. Current observations of Type Ia SNe has put constraints on the Einstein state parameters such as the matter density and the energy density of the universe, and has supported the Dark Energy cosmological parameter as the most likely candidate for causing the accelerated expansion of our universe.

Table 1. The calibrated and S-corrected magnitudes of SN 2003hv at different epochs.

JD	U	Error	B	Error	V	Error	R	Error	I	Error
892.88	12.191	0.015	12.460	0.015	12.464	0.015	12.439	0.015	12.797	0.015
896.78	12.737	0.015	12.717	0.015	12.586	0.015	12.622	0.015	13.057	0.015
899.79	13.196	0.017	13.050	0.015	12.774	0.015	12.910	0.015	13.346	0.015
906.80	14.414	0.015	14.032	0.015	13.273	0.015	13.148	0.015	13.233	0.015
910.76	14.902	0.015	14.584	0.041	13.545	0.034	13.279	0.035	13.131	0.037
914.70	15.272	0.032	15.024	0.066	13.924	0.033	13.600	0.034	13.291	0.052
917.75	15.445	0.015	15.215	0.015	14.108	0.015	13.817	0.015	13.517	0.015
920.74	15.613	0.025	15.359	0.029	14.327	0.024	14.068	0.031	13.791	0.037
923.72	15.699	0.022	15.472	0.015	14.455	0.015	14.231	0.015	13.972	0.015
926.75	15.801	0.022	15.575	0.015	14.586	0.015	14.384	0.015	14.150	0.015
929.72	15.941	0.015	15.646	0.015	14.688	0.015	14.473	0.015	14.279	0.015
932.67	15.991	0.015	15.721	0.015	14.781	0.015	14.615	0.015	14.451	0.015
939.71	16.217	0.024	15.886	0.015	15.011	0.015	15.864	0.015	14.788	0.025
946.71	16.378	0.029	16.007	0.015	15.211	0.015	15.104	0.015	15.091	0.015
953.72	16.506	0.058	16.144	0.018	15.408	0.020	15.334	0.015	15.386	0.015

Column 1 is Julian Date minus 2,452,000. The time of B-band maximum is JD 891.7

Table 2. The $\Delta M_{15}(B)$ and the absolute magnitudes of 31 SNe (z>0.01) from Hicken et al. (2009).

Supernova (z > .01)	$\Delta M_{15}(B)$	error	mU	error	E_{U-B}	error
97E	1.41	0.09	14.77	0.1	0.0355	0.0213
98bp	1.96	0.08	15.2	0.08	0.0104	0.0084
99aa	0.8	0.06	14.17	0.06	0.0104	0.0088
99dk	1.19	0.05	14.54	0.09	0.1052	0.0242
99dq	0.86	0.11	13.88	0.1	0.1249	0.0213
99ee	0.9	0.03	14.65	0.03	0.2685	0.0171
99gp	0.8	0.07	15.4	0.06	0.0622	0.0184
01V	0.65	0.15	14.01	0.09	0.0714	0.0171
02dp	1.12	0.06	14.16	0.06	0.1119	0.00376
02hu	1.04	0.07	16.08	0.05	0.0151	0.0125
03W	1.16	0.04	15.6	0.08	0.1378	0.0209
05el	1.23	0.11	14.28	0.1	0.005	0.0054
05eq	0.86	0.11	15.77	0.08	0.0435	0.0196
05hc	0.97	0.05	16.93	0.06	0.048	0.0217
05iq	1.05	0.1	16.3	0.19	0.0129	0.0109
05kc	1.24	0.19	15.49	0.11	0.2606	0.0309
05lz	1.35	0.19	17.33	0.1	0.0723	0.0284
05mc	1.87	0.11	17.14	0.06	0.0322	0.0213

Table 2. Continued.

Supernova (z >.01)	ΔM_{15}(B)	error	mU	error	E_{U-B}	error
05ms	0.79	0.07	15.7	0.04	0.0293	0.0167
05mz	1.96	0.14	16.32	0.13	0.1111	0.0372
06ax	1.08	0.05	14.47	0.05	0.0159	0.0121
06az	1.3	0.06	15.87	0.06	0.005	0.005
06cc	1.01	0.05	17.6	0.06	0.3391	0.0213
06gr	0.95	0.13	16.59	0.09	0.1269	0.0217
06le	0.85	0.27	14.26	0.32	0.0317	0.0251
06oa	0.98	0.18	17.46	0.08	0.0777	0.028
06ob	1.7	0.12	17.78	0.08	0.0088	0.0088
06S	0.91	0.04	16.34	0.05	0.1119	0.0192
07co	1.14	0.09	16.39	0.1	0.1637	0.0288
08bf	1.01	0.09	15.29	0.08	0.0426	0.0204

REFERENCES

Arnett D. 1999, ApJ, 990, 8169

Bailey, S., Aldering, G., Antilogus, P., Aragon, C., Baltay, C., et al. 2009, A&A, 500, L17

Branch, D., & Tammann, G.A.1992, A&A, 30,359-89

Cardelli J. A., Clayton G. C., & Mathis J. S. 1989, ApJ, 345,245

Cousins, A.W.J. 1981, S. Afr. Astron. Obs. Circ, 6, 4

Elias, J. H., Matthews, M., Neugebauer, G., & Person, S. E. 1985, ApJ, 296, 379

Filippenko, A. V., Richmond, M. W., Matheson, T., Shields, J. C., Burbidge, E. M., et al. 1992a, ApJ, 384, L15

Foley, R. J., Chornock, R., Filippenko, A.V., Ganeshalingam, M., Kirshner, R. P., et al.2009a, Astron.J, 138, 376

Garnavich, P. M., Bonanos, A. Z., Krisciunas, K., Jha, S., Kirshner, R. P., et al. 2004, ApJ, 613, 1120

Goobar, A., & Perlmutter, S. 1995, ApJ, 450, 14

Hamuy, M., Phillips, M. M., Suntzeff, N. B., Schommer, R. A., Maza, J., et al. 1996a, Astron.J, 112, 2408

Hicken, M., Challis, P., Jha, S., Kirshner, R. P., Matheson, T., et al. 2009, ApJ, 700, 331

Jensen, J. B., Tonry, J.L., Barris, B.J., Thompson, R. I., Liu, M. C., et al. 2003, ApJ, 583, 712

Jha S., Riess A. G., & Kirshner R. P. 2007, ApJ, 659, 122

Johnson, H. L., Iriarte, B., Mitchell, R. I., & Wisniewski, W. Z. 1966, CoLPL, 4, 99

Kasen, D., Ropke, F. K., & Woosley, S. E. 2009, Nature, 460, 869

Kessler, R., Becker, A. C., Cinabro, D., Vanderplas, J., Frieman, J. A., et al. 2009, ApJS, 185, 32

Krisciunas, K., Suntzeff, N. B., Candia, P., Arenas, J., Espinoza, J., et al. 2003, Astron. J, 125, 166

Krisciunas, K., Phillips, M.M., Suntzeff, N. B., Persson, S. E., Hamuy, M., et al. 2004b, Astron.J, 127, 1664

Krisciunas, K., Garnavich, P. M., Stanishev, V., Suntzeff, N.B., Prieto, J. L., et al. 2007, Astron.J, 133, 58

Landolt, A. U. 1992, Astron.J, 104, 340

Landolt, A. U. 2007, Astron.J, 133, 2502

Leibundgut, B., & Suntzeff, N. B. 2003, ed. K. Weiler, Heidelberg, Springer, 77

Leibundgut, B. 2001, ARA&A, 39, 67

Leloudas, G., Stritzinger, M. D., Sollerman, J., Burns, C. R., Kozma, C., et al. 2009, ApJ, 1201, 5393

Mazzali, P. A., Maurer, I., Stritzinger, M., Taubenberger, S., Benetti, S., et al. 2011, ApJ, 1105, 1298

Meikle, W. P. S. 2000, MNRAS, 314, 782

Minkowski, R.1941, Publ. Astron. Soc. Pac, 53,224-25

Oke, J. B., & Sandage, A. 1968, ApJ, 154, 21

Nugent, P., Phillips, M., Baron, E., Branch, D., & Hauschildt, P. 1995, ApJ, 455, L147

Perlmutter, S., Aldering, G., Goldhaber, G., Knop, R. A., Nugent, P., et al. 1999, ApJ, 517, 565

Phillips M. M. 1993, ApJ, 413, L105

Phillips, M. M., Lira, P., Suntzeff, N. B., Schommer, R. A., Hamuy, M., et al. 1999, Astron.J, 118, 1766

Riess, A. G., Filippenko, A. V., Challis, P., Clocchiatti, A., Diercks, A., et al. 1998, Astron.J, 116, 1009

Riello, M., & Patat, F. 2005, Roy.Astron.Soc, 362,671-80

Ruiz–Lapuente, P., 2003, ApJ, 0304108

Stanishev, V., Goobar, A., Benetti, S., Kotak, R., Pignata, G., et al. 2007, A&A, 469, 645

Stritzinger, M., Hamuy, M., Suntzeff, N. B., Smith, R. C., Phillips, M. M., et al. 2002, Astron.J, 124, 2100

Timmes, F. X. & Swesty, F. D. 2000, ApJS, 126, 501

Tonry, J. L., Dressler, A., Blakeslee, J. P., Ajhar, E. A., Fletcher, A. B., et al. 2001, ApJ, 546, 681

Wang, L., Strovink, M., Conley, A., Goldhaber, G., Kowalski, M., Perlmutter, S., & Siegrist, J. 2005, ApJ, 635, L33

Wang, X., Wang, L., Pain, R., Zhou, X., Li, Z., et al. 2006, ApJ, 645, 488

CONTACT INFORMATION

Name: Deepak Bastola

Contact Address: c/o Dr. Kevin Krisciunas
Texas A & M University
Department of Physics & Astronomy
4242 TAMU
College Station, TX 77843-4242

Email Address: deepak613@neo.tamu.edu

Education: Bachelor of Science in Physics and Mathematics, May 2013
Texas A&M University
Undergraduate Research Scholar 2012